THE ANTIPROTON TARGET STATION ON THE BASIS OF LITHIUM LENSES

B.F.Bayanov, A.D.Chernyakin, V.N.Karasyuc, G.I.Silvestrov, T.A.Vsevolozhskaya, V.G.Volohov, G.S.Willewald

Institute of Nuclear Physics, Novosibirsk, USSR

ABSTRACT

In the paper we describe the project of an antiproton target station with particle focusing carried out with lithium lenses. The optimal conditions of obtaining high particle density inside a phase volume determined by the following antiproton cooling for three projects - Precooler (FNAL), Antiproton Accomulator (CERN) and INF-IHEP (USSR) are analysed. The efficiency of antiproton collection with a lithium lense is compared to the efficiency achieved with another focusing devices - magnetic horn and quadrupole triplet.

In all antiproton storage ring projects, the major problem of optimizing antiproton production conditions is the achievement of maximum phase density of particles in the phase volume determined by the requirements of a subsequent beam cooling. For this purpose, the geometrical parameters of a target, its material, and the conditions of proton beam focusing and antiproton collection should be optimized. The present paper concerns the optimal targetry conditions for three designs of antiproton storage rings - Precooler (FNAL), Antiproton Accumulator (CERN), and Antiproton Source for the IHEP Acceleration-Accumulator Facility (INP) and also the efficiency of antiproton collection by various optic devices.

The optimal targetry conditions analysis

The antiproton beam parameters at the target entrance are mainly determined by the antiproton production angles and a target length. The production angles distribution may be considered as a Gaussian one with the mean square $\langle\theta^2\rangle \cong \frac{2mm_\pi c^2}{p^2}$, m_π is the pion mass, m and p are the antiproton mass and momentum). This follows from the thermodynamical description of the antiproton transverse momentum distribution at $T \cong m_\pi c^2$. This description agrees well enough with experimental data at relatively small angles. The antiproton distribution in a transverse phase space may be characterized by the effective values of an emittance $\varepsilon_{\bar{p}}$ and α and β - functions, which are determined by the mean squares of angles and coordinates, $\langle\theta^2\rangle$ and $\langle r^2\rangle$, and by the product $\langle r\theta\rangle$ at the target entrance as $\varepsilon_{\bar{p}} = \sqrt{\langle r^2\rangle\langle\theta^2\rangle - \langle r\theta\rangle^2}$, $\beta_{\bar{p}} = \frac{\langle r^2\rangle}{\varepsilon_{\bar{p}}}$, $\alpha = -\frac{\langle r\theta\rangle}{\varepsilon_{\bar{p}}}$. The values $\langle r^2\rangle$ and $\langle r\theta\rangle$ are $\langle r^2\rangle \cong \frac{\langle\theta^2\rangle z^2}{3}$ and $\langle r\theta\rangle \cong \frac{\langle\theta^2\rangle z}{2}$, where z is the target length.

The effective emittance of the antiproton beam and the minimum value of its β - function (at the centre of the target) are: $\varepsilon_{\bar{p}} \cong \frac{\langle\theta^2\rangle z}{2\sqrt{3}}$ and $\beta_{\bar{p},min} = \frac{z}{2\sqrt{3}}$. The antiproton yield is maximum when the target length is close to the nuclear absorption length λ . At $z = \lambda$, the emittance

be considered as an effective emittance of antiproton production, $\varepsilon_0 = \frac{\langle\theta^2\rangle\lambda}{2\sqrt{3}}$. The capture efficiency at a given acceptance ε may be characterized by the function F determined by the relation of the acceptance to the antiproton beam emittance, the degree of proton and antiproton absorption inside the target. The number of captured antiprotons per incident proton is determined by means of this function as $\frac{\Delta N_{\bar{p}}}{N_p} = \frac{1}{\sigma_{in}} \cdot \frac{d\sigma}{dp} \cdot F \cdot \Delta p = \frac{1}{\sigma_{in}} \cdot \frac{d^2\sigma}{dp d\Omega} \pi \langle\theta^2\rangle F \cdot \Delta p$.

Analytical evaluation of the capture efficiency into the acceptance under condition that $\varepsilon \ll \lambda\langle\theta^2\rangle$ and the acceptance envelope function β equals to that of an antiproton beam $\beta_{\bar{p}}$, determines the optimal target length z_{opt} as $z_{opt} \cong 1.3\sqrt{\frac{\varepsilon\lambda}{\langle\theta^2\rangle} + \frac{r_0^2\lambda}{\varepsilon}}$ and corresponding value of F as:

$$F \cong \frac{8}{3} \cdot \frac{\varepsilon \cdot \exp(-\frac{z_{opt}}{\lambda})}{\langle\theta^2\rangle(\lambda + z_{opt})}$$

Here r_0 is the radius of a proton beam with the uniform particle density. The thin proton beam condition is $r_0^2 \ll \frac{8}{3}\frac{\varepsilon^2}{\langle\theta^2\rangle}$. The optimal antiproton collection angle is determined by a minimum value of β - function of the acceptance $\beta_{min} = \beta_{\bar{p},min} = \frac{z_{opt}}{2\sqrt{3}}$, and it equals to $\alpha_{max} \cong 1.65\left(\frac{\varepsilon}{\lambda}\langle\theta^2\rangle\right)^{1/4}$. The expression for $\frac{\Delta N_{\bar{p}}}{N_p}$ is $\frac{\Delta N_{\bar{p}}}{N_p} \cong \frac{1}{\sigma_{in}} \cdot \frac{8}{3}\pi\varepsilon\Delta p \cdot \frac{d^2\sigma}{dp d\Omega} \cdot \frac{\exp(-\frac{z_{opt}}{\lambda})}{z_{opt}+\lambda}$. In analytical evaluation of the capture efficiency we have not taken into account the multiple and elastic nuclear scattering of protons and antiprotons, the difference in their absorption lengths, the angular spread, and the inhomogeneities of the proton coordinate distribution in the initial beam. It has been done in computer simulation; its results (Fig. 1, a-d) are consistent with the analytical estimates. The values of F in Fig. 1A, b were calculated at optimal β_ε and z (tangsten) for each value of ε and r_0, in Fig. 1c - for optimal z. Shown in Fig. 1d is the F dependance on a target length (mercury) for targets with a large cross-section and with a cross-section equal to that of a proton beam (thin target). The proton beam β - function values for the data in Fig. 1c, d are: 1 cm (FNAL), 6 cm (CERN), 10 cm (INP). The main parameters characterizing the optimal targetry for three mentioned above projects are listed in Table 1.

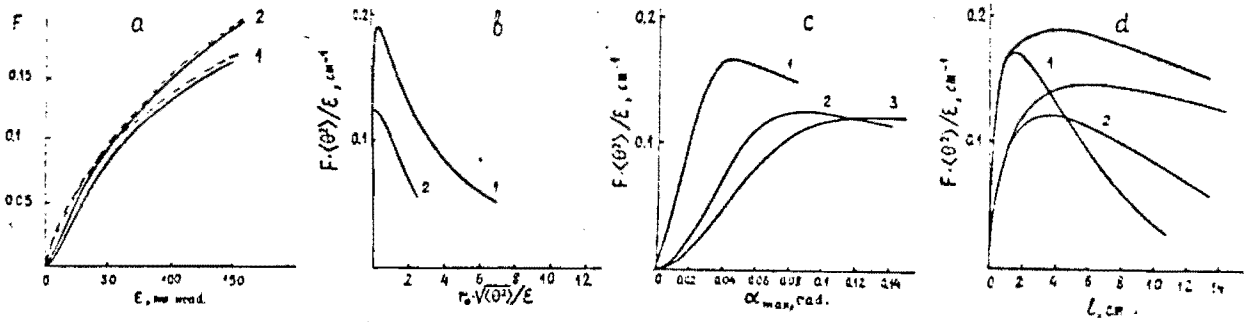

Fig. 1 Capture efficiency in the dependence on a) the acceptance size for the proton beam radius equal to 0.5 mm (1) and infinitely thin proton beam (2). Solid lines denote the simulation, dotted lines - analytical evaluation. The antiproton momentum is equal to 6 GeV; b) the proton beam radius for the FNAL (1) and AA (2) project; c) the collection angle from a target for the FNAL (1), INP (2), and AA (3) projects; d) the target length for the thick and thin targets at the uniform proton beam distribution, for FNAL(1), AA(2)

Table 1

	p GeV/c	ε mm·mrad	Δp/p	Target material	[illegible] cm	[illegible] mrad	F
FNAL[1]	4.5	5	±2	Hg/W	1.5	35	0.0064 / 0.0086
CERN[2]	3.5	100	±0.75	Hg/W	3.5	100	0.053 / 0.066
INP[3]	5.5	60	±3.2	W	3.5	80	0.80

Antiproton collection

Antiproton collection up to the optimal angle requires powerful optic systems. The choice of a collecting lens (quadrupoles, "magnetic horns", lithium lenses) is determined both by angular acceptance and aberrations, among which the chromatic aberration needs the great care.

The chromatic dispersion of particle deflection angles in a lens leads to an additional angular spread in the beam. If the beam transfer with an optical system is described with a matrix (M) as $(X)=(M)(X_0)$, the angular and coordinate increase at its entrance due to chromatic aberration (ΔX) is described by the matrix (M') obtained by differentiation of (M) over momentum, as $(\Delta X)=\frac{\Delta p}{p}(M')(X_0)$. The effective angular and coordinate increase in a beam source (ΔX_0) is determined as $(\Delta X_0)=(M)^{-1}(\Delta X)=\frac{\Delta p}{p}(M_0')(X_0)$, where $(M_0')=(M)^{-1}(M')$. An increase of beam emittance is described by the expression:

$$\varepsilon=\varepsilon_0\sqrt{1+\left\langle\left(\frac{\Delta p}{p}\right)^2\right\rangle\left(a_{11}^2+a_{22}^2+a_{21}^2\beta_0^2+\frac{a_{12}^2}{\beta_0^2}\right)+\left\langle\left(\frac{\Delta p}{p}\right)^2\right\rangle^2\cdot\Delta^2}$$

where a_{ik} and Δ are the elements and determinant of (M_0'). For example, the use of a quadrupole triplet, proposed to collect antiprotons with the momentum spread $\pm 1.5\cdot10^{-3}$ in a preliminary FNAL project[4], at the momentum spread $\pm 2\cdot10^{-2}$ would lead to a decrease of the capture efficiency by a factor of 4, as shown by computer simulation. For a thin lens with focal distance f the aberration increase of an emittance is determined as $\varepsilon=\varepsilon_0\sqrt{1+\left\langle\left(\frac{\Delta p}{p}\right)^2\right\rangle\left(2+\frac{\beta_0^2}{f^2}+\frac{f^2}{\beta_0^2}\right)}$.

Thus, besides the main restriction - a relatively small collection angle (no more than 0.01-0.02 rad), chromatic aberration turns out to be an additional restriction on the use of quadrupoles for antiproton collection.

The use of the systems with large magnetic fields and axisymmetric focusing of the parabolic lense (magnetic horn) or lithium lens type allows the angular acceptance to be extended up to optimal collection angles. The losses due to multiple scattering are minimized, in this case, by short focal lengths and minimum material thickness. Unfortunately, the nuclear interaction can limit the applicability of such systems in some cases.

Fig. 2 shows the profiles of possible variants of parabolic lenses for antiproton collection in the optimal angle in all three projects. These lenses have the focal distances, fields, and the wall thicknesses close to the limiting. The currents in the lenses are: 110 kA (FNAL), [illegible] kA (CERN),

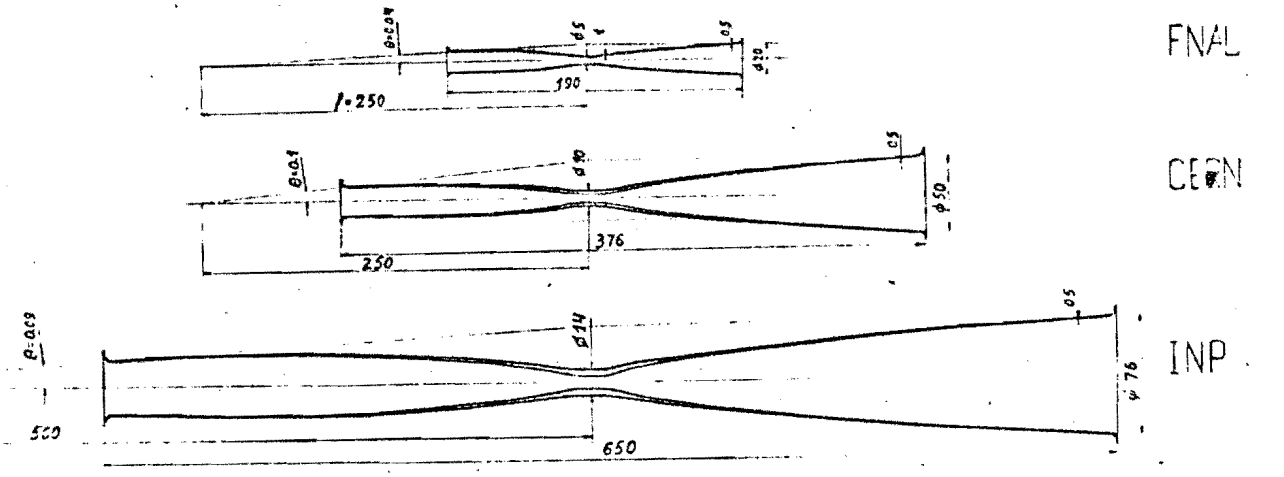

Fig. 2 Variants of parabolic lenses. Cross-section

400 kA (INP). The profile shapes are determined by the linear dependence of entrance coordinates on excit angles, that provides the minimum geometrical aberration[5]. The wall thickness changes with a distance from the axis as $\frac{1}{r}$ and is equal to 0.5 mm at maximum r . It corresponds to the mechanical stress $\sigma > 1200$ kg/cm^2 in the wall. The computer simulation of particles passage through aluminium lenses shows that the capture efficiency decreases by more than 4 times for the FNAL project (F = 0.0015) and by 1.65 times for the CERN project (F = 0.032). In the FNAL case the losses are mainly due to multiple scattering. The nuclear losses and chromatic aberration cause a decrease in efficiency of about 20%. In the CERN case, the decrease is largely (down to F = 0.036) due to nuclear losses.

An essential decrease of multiple scattering can be achieved with the use of lenses made of beryllium. The manufacturing process for beryllium lenses with the parameters close to those for FNAL and CERN projects has been developed in the INP[6]. In the FNAL case, the beryllium lens efficiency is about 2 times higher as compared to the aluminium one, i.e. the capture efficiency constitutes 0.5 from the maximum; in the CERN case, the gain is 6% only (up to F = 0.034).

Lithium lenses[7] can provide the minimum focal distance at which the distortion of the antiproton beam emittance is excluded nearly completely. For example, in the FNAL project the lens for antiproton collection in an optimal angle can have the 10 cm focal distance and the 0.8 cm aperture. In this case, the field on the surface is 12 T and the lens length is 6 cm. The angle of multiple scattering in the lithium and beryllium walls at the ends is $\sqrt{\langle\theta^2\rangle}$ = = $7 \cdot 10^{-4}$ rad, that is less than the angular size of acceptance at the lens. Computer simulation shows that the losses in capture efficiency scarcely exceed nuclear losses in the lens. At INP the technology of lithium lenses has been developed, and wide experience has been gained in operation with similar systems[8]. At present, INP is designing the lens shown schematically in Fig. 3. It has aperture 2 cm, length 10 cm, and can be fed by a 300 mks current pulse

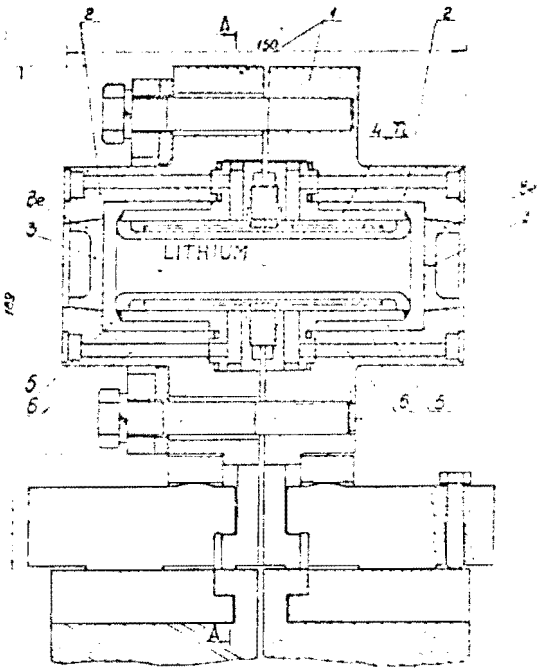

Fig. 3 The antiproton lithium lens cross-section: 1-flat current input; 2 - current connection cups; 3 -beryllium windows; 4 - titanium envelope of the lens, 5 - lithium axisymmetric current input; 6 - water cooling system.

of up to 700 kA through a matching transformer. Change in innermost structure (position 4 in Fig. 3) and corresponding change in the amplitude and pulse duration make it possible to use this lens in all three projects.

The focal distance of the collecting lens has a lower limit due to a burning through the beryllium entrance wall of the lens by a proton beam with high density near the target. Heating estimates and the FNAL neutrino beam experience with beryllium targets show that at an intensity of $3 \cdot 10^{13}$ protons per pulse and a millimeter beam size beryllium is not destroyed. To have such a size at a distance of about 7 cm from the target center, the proton beam should have large divergence achieved by strong focusing of it on the target. The lithium lens with the 35 cm focal distance and the 0.5 cm aperture meets this condition. For 80 GeV it has length 13 cm and field 15 T. At present, such a lens is undergoing a test at INP.

Proton focusing on a target and antiproton collection with lithium lenses with the above parameters results, for the FNAL project, in a capture efficiency constituting the $\sim$ 0.75 of the ideal value (Table I). If, because of the collecting lense entrance wall heating, it is necessary to shift it up to the focal distance of 20 cm, the scattering contribution decreases the collection efficiency down to $F = 0.0035$. This is only 10% higher than for the beryllium horn.

The target device

At intense proton beams (more than 10^{13} particles per pulse) and small beam sport sizes the work with heavy targets is accompanied by a large energy release (of the order of a few kJ) and high temperature of pulse heating; the latter leads to the explosive regime of a target operation. One of the ways to overcome the difficulties is the use of liquid-metallic, for example mercury, targets. This enables one to replace a target between pulses and to solve the problem of target cooling. After consideration of several variants of mercury targets we have chosen a flat-jet-like target. The jet flows through a narrow slit and the level of mercury is maintained constant with a pump. If the mercury level above the slit is 1-2 cm, the jet turns out to

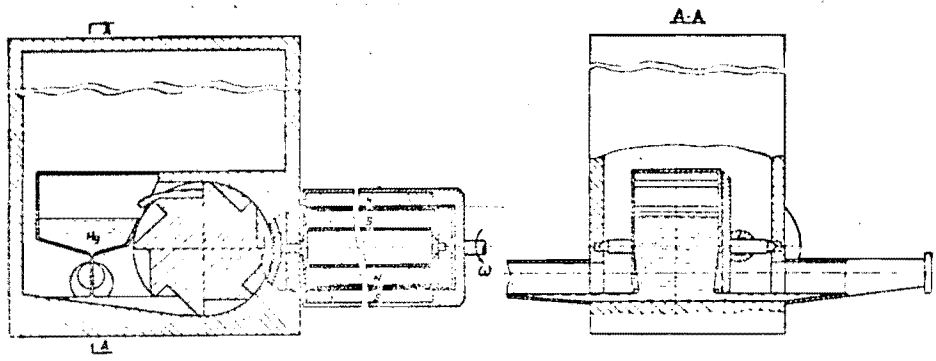

Fig. 4 Schematic cross-section of mercury pumps.

well-shaped with the stable cross-section. In studing of the mercury jet flow from a narrow slit of 60 cm long its width was ranged from 0.5 to 3 mm. After analysing various designs of pumps for mercury pumping we have chosen simplest variant the principle of operation of which is demonstrated in Fig. 4. The trials of the models of these pumps showed that, it can provide pump capacity more 5 liters per minute, sufficient for creating a stable jet with 60 x 3 mm^2 cross-section. This construction is placed in the air-tight containers with water cooling. The beam is passed through the exit and entrance windows covered with beryllium foils.

ATS layout

The use of short focusing lenses with small apertures allows a very compact antiproton target station (ATS) to be built up. The station scheme is shown in Fig. 5. All components of the station are placed on one common platform (4), 2 m long, and 0.7 m wide: a lithium lens for proton focusing (5), a target device (3), a lens for antiproton collection (2), and a bending magnet with the 5 T field. The platform can move along a stationary plate (10) together with the mobile section of shielding (7). As a plug, the latter enter the window of a stationary shielding (8,16) under operation of the ATS. Both lenses and separating magnet, with their matching transformers are installed on the platform and have radiation hard insulation. The transformers have a low-inductance current inputs (17) which pass through the mobile shielding. The current inputs are connected to a remotely-operated switch (15). Each element can be lifted up and shifted with a special manipulator for replacement. To do this, each element is mounted on the special catches and remotely-operated current and water connections. Both lenses can be remotely-adjusted simultaneously with an accuracy better than 100 microns.

The ATS will be mounted at IHEP for a study of the behaviour of solid and liquid metallic targets in the explosive regime at the 70 GeV proton beam and also for solution of a number of problems concerning the performance of a complex physical equipment at very high levels of radiation.

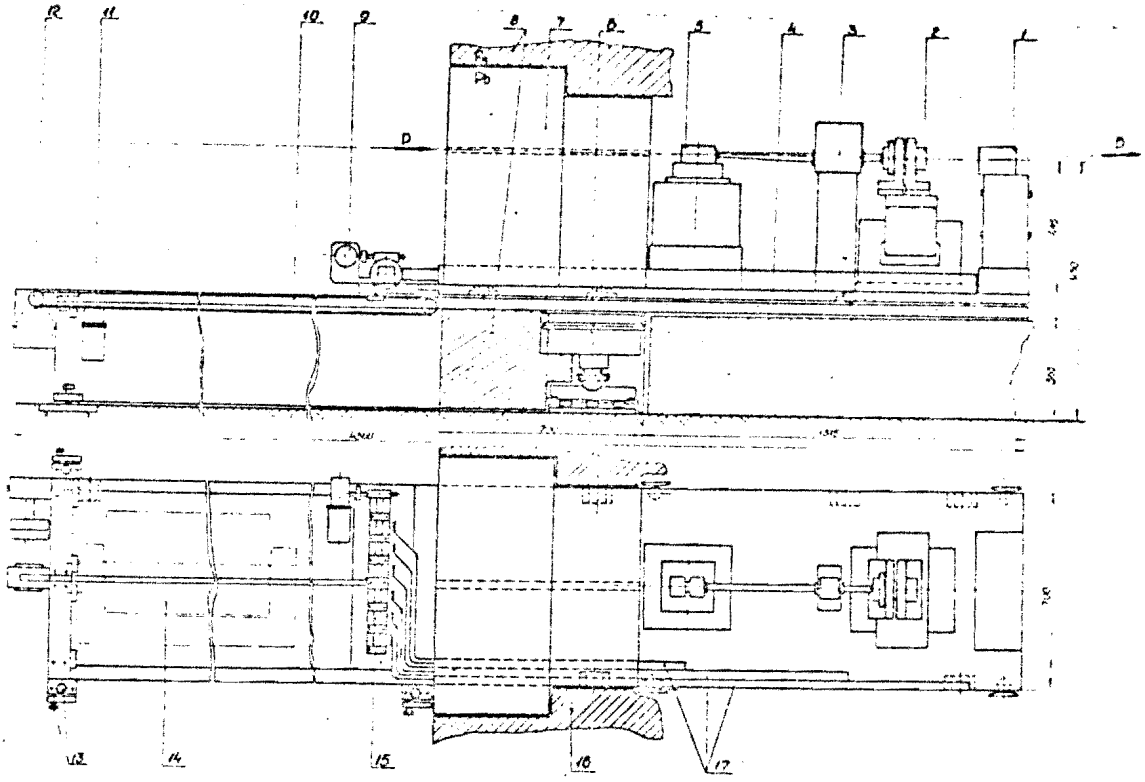

Fig. 5 ATS layout. 1 - bending magnet, 2 - antiproton lens, 3 - target device, 4 - mobile platform, 5 - proton lens, 6 - distant adjusting device of the ATS, 7 - mobile shielding, 8 and 16 - stationary shielding, 9 - switch-drive, 10 - stationary plate, 11 - chain belt, 12 - drive mechanism, 13 - adjusting devices, 14 - the second matching transformers, 15 - current switches, 17 - radiation hard current inputs.

* * *

REFERENCES

1. Design report. The Fermilab high-intensity antiproton source, FNAL, October, 1979.
2. Design study of a proton-antiproton colliding beam facility, CERN/PS/AA, 78-3, 27.1.1978.
3. T.A.Vsevolozhskaya et al., "An antiproton source for the IHEP acceleration-accumulation fecility. INP Report, May 1980.
4. Beam Transport and Target System for pp and $p\bar{p}$ Colliding Beams, FNAL 06/20/78.
5. T.A.Vsevolozhskaya, G.I.Silvestrov, ZhETF, XLIII, 61, 1973.
6. G.S.Willewald, V.N.Karasyuk, G.I.Silvestrov, ZhETF, XLVIII, 566, 1978.
7. T.A.Vsevolozhskaya, M.A.Lyubimova, G.I.Silvestrov, ZhETF, XLV, 2494, 1975.
8. B.F.Bayanov, G.I.Silvestrov, ZhETF, XLVIII, 100, 1978.